ISSN 2618-1584 Vol. 7, Issue 6: 125-140, DOI: 10.25236/FMSR.2025.070616

Dissecting Causal Relationships between Metabonomics, Circulating Plasma Proteomics, and Lumbar Disc Herniation: A Mendelian Randomization Study

Linhan Qin[1,a], Qinghua Ding[1,b,*]

[1]*Department of Orthopedics, The Fourth Affiliated Hospital of Anhui Medical University, Hefei, Anhui, China.*
[a]*2345012242@stu.ahmu.edu.cn,* [b]*ch2003640001@fy.ahmu.edu.cn*
**Corresponding author*

Abstract: *Lumbar disc herniation (LDH) is a prevalent spinal disorder. Although empirical investigations have indicated correlations between circulating proteins/metabolites and LDH, their causal roles remain unclear. To elucidate these potential causal relationships, we employed Mendelian randomization (MR) methodology. Specifically, we conducted a comprehensive two-sample MR study to assess the causality of 4,907 circulating proteins and 1,400 plasma metabolites on LDH risk within a European-ancestry population. We validated significant associations using sensitivity analyses (weighted median, MR-Egger, MR-PRESSO) and consolidated primary findings via comprehensive analysis with multiple-testing-corrected thresholds. Then, reverse MR analysis was used to test for bidirectional causal relationships between LDH and the identified proteins. This was followed by the construction of a protein-protein interaction network and enrichment analysis, aimed at deciphering the biological relevance of these proteins to LDH. Genetic instruments for the circulating proteins were derived from a large-scale pQTL (protein quantitative trait loci) investigation involving 35,559 individuals, which provided data on 4,907 proteins. Data for plasma metabolites were obtained from a relevant GWAS of 14,296 subjects. Meanwhile, summary statistics for LDH were sourced from the large-scale FinnGen R12 database. Our analysis identified 44 plasma proteins and 23 plasma metabolites with putative causal effects on LDH. For the most significant results derived from the two sets of MR analyses, the inverse-variance weighted method was applied, followed by a meta-analysis. Subsequent pathway analysis delineated four key metabolic pathways, unveiling promising therapeutic targets for LDH intervention (ENPP2, FTMT, PAPOLG).*

Keywords: *Causality verification, blood metabolites, plasma proteins, multi-omics, lumbar disc herniation, Mendelian randomization analysis, metabolic pathway analysis*

1. Introduction

Lumbar disc herniation (LDH) is a prevalent spinal disorder mostly resulting from degenerative alterations or external impacts. The syndrome results in the nucleus pulposus herniating through the annulus fibrosus into the spinal canal, subsequently compressing the nerve roots or spinal cord. This leads to many clinical manifestations, such as lumbar discomfort, radicular leg pain, paraesthesia, muscular weakness, and failure of bowel or bladder control.[1] Annually, around 50 individuals per 1000 are newly diagnosed with LDH, corresponding to an approximate global incidence rate of 5%. The lifetime prevalence is estimated at 2% to 3%, suggesting that 2 to 3 persons per 100 will encounter LDH at some stage in their lives.[2] Researchers have determined that the morbidity of LDH is somewhat greater in males than in women, with a male-to-female ratio ranging from around 1.2:1 to 1.5:1. Construction workers, chauffeurs, and office personnel are among the occupations that are associated with an elevated risk of developing LDH. These occupations are characterized by protracted sitting or standing, significant physical exertion, and repetitive actions such as bending and lifting.[3–5] A combination of critical pathological processes is the principal cause of LDH development. Intervertebral degeneration of discs is a critical element, as the water content of the pulposus nuclei diminishes with age, leading to a reduction in their suppleness and ability to absorb mechanical strain. The degeneration of the annulus fibrosus is a critical element; over time, the fibrous outer circle thins and becomes more

ISSN 2618-1584 Vol. 7, Issue 6: 125-140, DOI: 10.25236/FMSR.2025.070616

susceptible, hence elevating the likelihood of ripping and allowing the nucleus pulposus to herniate through the compromised region.[6,7] The pathogenesis of LDH involves a combination of mechanical, metabolic, genetic, and inflammation-related factors. Prolonged mechanical strain and incorrect body position, including extended standing, sitting, or constantly bending, can impose too much pressure on the lumbar vertebral discs, resulting in disc rupture and protrusion. Annulus fibrosus tears may also be the consequence of acute trauma, such as the abrupt raising of heavy objects or tumbles, allowing the nucleus pulposus to herniate into the spinal canal and pressure neuronal tissues. Furthermore, genetic susceptibility is acknowledged as an important danger factor, with those possessing relatives with a history of LDH demonstrating increased sensitivity.[8]In addition, alterations in the biochemical constituents of lumbar discs, such as proteoglycans and collagen fibers, drive structural and functional changes within the disc. Also, the protrusion of the nucleus pulposus can trigger a localized inflammation response, which results in the release of numerous mediators of inflammation that exacerbate compression of the nerve root and injury.[9]

The pathophysiological changes of the LDH include the following: The nucleus pulposus protrudes through the ruptured annulus fibrosus into the spinal canal, applying direct pressure on the nerve roots or spinal cord, leading to discomfort and dysfunction.[10] Neural root entrapment transpires when the protruding nucleus pulposus applies pressure on the neural roots, resulting in edema, inflammation, and ischemia, which manifest as muscular weakness, numbness, and radiated pain.[11] On the other hand, the degenerative modifications and intervertebral disc herniation disrupt spinal stability, potentially contributing to the compromise of spinal stability and alignment, hence aggravating symptoms.[12] Disc herniation can cause discomfort and dysfunction, leading to reflex spasm of the lower back muscles, which intensifies pain and restricts mobility.[13]

For LDH, management strategies focus on two aspects: prevention through weight control, proper posture, and tailored exercise; and treatment, which ranges from conservative care to surgery.[14–19]

Metabolomics and proteomics have gained recognition in recent years for their capacity to elucidate the molecular complexities of LDH, presenting identifying potential therapeutic targets. Metabolomic sequencing and bioinformatics have identified distinct metabolic and proteomic changes in LDH, primarily related to inflammation-mediated pathways and amino acid metabolism, in the context of a preliminary, exploratory investigation. Plasma proteomic profiling in patients with lumbar disc herniation has uncovered marked perturbations in specific protein expression patterns and antioxidant metabolic processes, underscoring their potential utility as biomarkers and mechanistic mediators in the pathogenesis of lumbar disc herniation and its associated complications. Currently, research mostly focuses on association studies, with a burgeoning interest in exploring causal relationships.

To date, there is scant direct study on the causal link among metabolites, proteins, and LDH; nonetheless, available studies suggest that metabolites and proteins significantly contribute to disc degradation and inflammatory responses. The distinct functions of various metabolites and protein phenotypes in LDH are inadequately investigated, as the majority of research emphasises general processes and mechanisms of inflammation, neglecting comprehensive analyses of phenotypic variations, functional characteristics of diverse cytokines, and how they interact with the disease level of severity. This gap raises unanswered concerns regarding the precise metabolites and proteins essential for disease development, the presence of high-risk phenotypes, and the differential impacts of various metabolite and protein phenotypes in patients.

Recent years have seen advancements in research on gene polymorphisms associated with LDH, utilizing methodologies such as genome-wide association studies (GWAS) and single-gene analyses. The results of these investigations indicate that some gene polymorphisms may elevate the risk for developing LDH by influencing extracellular matrix metabolism or related signaling pathways in intervertebral discs.[20] Large-scale GWAS on human genotype data offer novel insights into the genetic variations linked to LDH, thereby improving our comprehension of the disease's genetic foundation. In addition, gene polymorphisms may modulate inflammation-related genes, thereby affecting the expression and release of metabolites and proteins that are essential for the inflammatory response in disc degeneration.[21]

MR employs genetic variation to furnish instrumental factors for exposure assessments, hence evaluating the causal relationship between exposure and outcomes.[22–24] The stochastic distribution of alleles, unaffected by traditional confounders, supports these causal claims.[25] Accordingly, the present study will make use of publicly available GWAS data to identify potential causality between the plasma proteome, metabolome, and LDH. A preliminary two-sample Mendelian randomisation strategy will determine the causal relationships among the proteome, metabolome, and LDH. A subsequent analysis

ISSN 2618-1584 Vol. 7, Issue 6: 125-140, DOI: 10.25236/FMSR.2025.070616

of metabolic pathways assessment will elucidate the intricate interactions between the proteome and metabolome in the context of LDH.

In this study, we leveraged GWAS data and integrated Mendelian randomization (MR) analysis with meta-analytic approaches to investigate the potential causal relationships between 4,907 proteins, 1,091 plasma metabolites, and LDH. The objective is to uncover the causal interactions between certain proteins and metabolites with LDH, propose potential pathogenic mechanisms, and offer novel pathways for the development of tailored therapy solutions centred on these metabolites and proteins.

2. Methods and materials

2.1. Study design

This study used a two-sample Mendelian Randomisation (TSMR) paradigm to examine the causal links among the plasma proteome, metabolome, and LDH in a European cohort. Data was obtained from a variety of repositories. The three primary assumptions of MR analysis were rigorously adhered to during the research procedure in this paper: 1) We screened using a threshold p-value of less than 5×10-8, as single-nucleotide polymorphisms (SNPs) are significantly correlated with exposure factors. 2) We excluded SNPs that were significantly correlated with other LDH-related exposures, so SNPs would not be affected by confounding factors. 3) The exposure factor is the sole mechanism by which SNPs can influence the outcome. Consequently, SNPs influence LDH (the outcome of this study) solely by mediating the exposure (plasma proteins or metabolites).[26]

After identifying positive causal linkages, we examined the interaction between the plasma proteome and metabolome concerning LDH, employing a metabolic pathway analysis. In parallel, we also performed enrichment analysis following the construction of the differential protein-protein interaction (PPI) network. The study entails the examination of data from the GWAS database; hence, an ethical evaluation is unnecessary. A flowchart Fig.1) was developed to elucidate the research process.

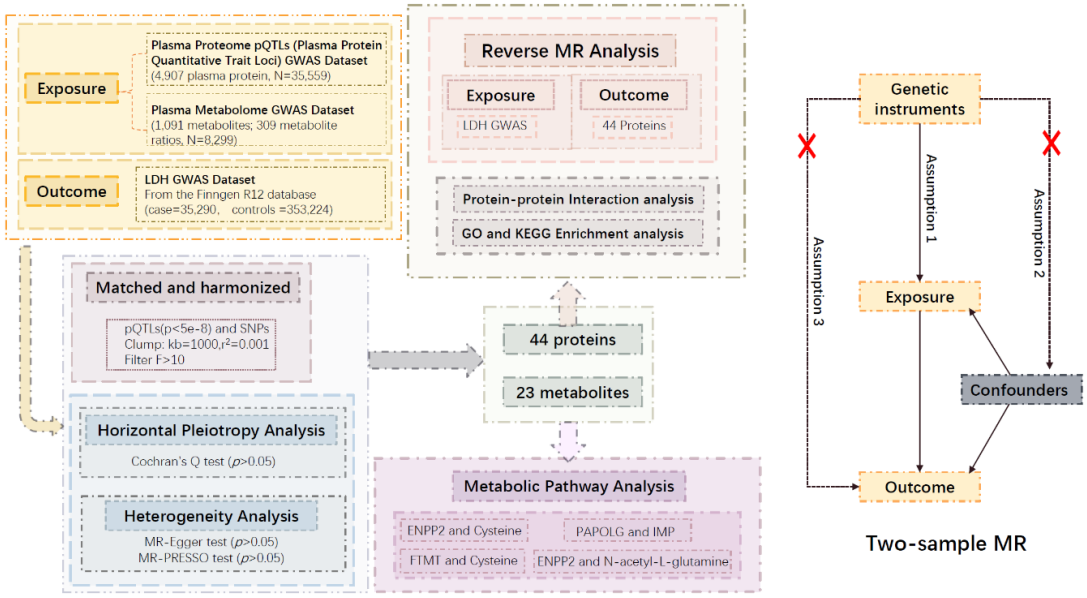

Figure 1: The flowchart of the study.

2.2. Data source

2.2.1. Plasma Proteome GWAS Dataset

The plasma proteomic data were derived from a GWAS conducted in 35,559 participants of the Icelandic Decode cohort.[27] This study assessed 4,907 plasma protein concentrations using the SomaScan aptamer-based test, which evaluated 4,907 aptamers directed at 4,719 unique proteins. Genotyping was conducted on all participants, and comprehensive phenotypic data was compiled. The subsequent integration of genetic data with protein measurements facilitated the identification of associations between genetic variants and protein expression levels, which are classified as protein quantitative trait

ISSN 2618-1584 Vol. 7, Issue 6: 125-140, DOI: 10.25236/FMSR.2025.070616

loci (pQTL).[28] Overall, 18,084 pQTL associations were identified through this analysis.

2.2.2. Plasma Metabolome GWAS Dataset

The GWAS dataset for the plasma metabolome was obtained from the Canadian Longitudinal Study of Ageing (CLSA), which includes 8,299 European individuals. The study cohort comprised unrelated European individuals aged 45 to 85 years to reduce any bias in demographic stratification. To mitigate bias in the analysis, Europeans with first- and second-degree relatives were excluded using kinship-based inference from the KING package (https://www.kingrelatedness.com/manual.shtml).[29] This dataset comprised quantitative measurements of 1,091 metabolites categorised into nine groups: lipids, xenobiotics, nucleotides, carbohydrates, amino acids, cofactors and vitamins, energy substrates, peptides, and metabolites of unclear classifications.[30] These measurements were conducted using ultra-high-performance liquid chromatography-tandem mass spectrometry (UPLC-MS/MS). The data was subjected to uniform normalisation and noise reduction procedures after meeting the selection criteria of having less than 50% missing values. Furthermore, 309 metabolite ratios were obtained from the Human Metabolome Database (HMDB), which can be accessed at http://www.hmdb.ca/system/downloads/current/serum_metabolites.zip. The fastGWA algorithm was implemented in the GWAS analysis, which examined 1,400 metabolite profiles. Linear regression was employed to control for covariates such as sex, age, fasting duration, genotyping batch, and the first ten genetic principal components. We acquired GWAS data for the plasma metabolome from 1400 European samples in the GWAS catalogue (https://www.ebi.ac.uk/gwas/), with accession numbers spanning from ebi-a-GCST90199621 to ebi-a-GCST90201020.

2.2.3. LDH GWAS Dataset

In a separate research, it was shown that when the ancestry of the exposed cohort and the result were the same in the MR analysis, and the samples either did not overlap or overlapped by less than 10%, the bias from multiple variables was diminished in comparison to that of single-source samples. Consequently, the population samples used for the LDH cohort in this study do not intersect with the population exhibiting plasma proteomes and metabolites, thereby mitigating several possible biases. The GWAS dataset for LDH was procured from the Finngen R12 database, encompassing data on 35,290 LDH patients, 353,224 controls, and 21,325,323 SNPs. The data selection criteria included: prioritisation of higher sample numbers, assurance of representative data sources, and alignment of the research population with the exposure data.

2.3. Identification of Instrumental Variables (IVs)

Stringent criteria were employed to evaluate SNPs within the plasma proteome and metabolome as prospective genetic proxies and select them as instrumental variables (IVs). Initially, SNPs were required to exhibit robust associations in GWAS data, with p-values less than 5×10^{-8}. To reduce the probability of linkage disequilibrium, we utilized the TwoSampleMR software, establishing a clumping threshold of $r^2 = 0.001$ and a distance of 10,000 kilobases (kb), prioritizing SNPs with lower p-values during selection.[31,32] It is crucial to acknowledge that the selection of IV agents differed among plasma subgroups. The selection of strongly correlated instrumental variables in the protein subgroup was predicated on pQTLs located in both cis and trans regions. In contrast, the metabolome subgroup did not restrict the selection of SNPs with high correlation to transcribed regions, which facilitated the identification of more dependable protein-based drug targets.[33]

To mitigate the influence of weak IVs on the robustness of the MR analyses, we computed the F statistic utilizing the formula $F = (n - k - 1)/k \times (R^2/(1-R^2))$, which evaluates the strength of the IVs. Here, R^2 denotes the cumulative explained variance of the chosen SNPs, n represents the sample size, and k indicates the quantity of analyzed SNPs.[34] Only SNPs with an F value greater than 10 were preserved, a measure that helps exclude poor instruments and strengthens the reliability of the study findings.

3. Mendelian Randomization Analysis

We primarily employed TSMR to elucidate the interplay between the plasma proteome, metabolome, and LDH. Our analytical framework consisted of five unique MR tests: Inverse Variance Weighted (IVW), MR Egger, Weighted median, Simple mode, and Weighted mode. Specifically, the primary analytical instrument for assessing the relationship between multiple SNP proxies and LDH was the IVW random-effects model, while the Wald ratio was chosen as the primary method for investigating the association between single SNP proxies and LDH.[35] The stability and reliability of our findings were

ISSN 2618-1584 Vol. 7, Issue 6: 125-140, DOI: 10.25236/FMSR.2025.070616

significantly supported by the results obtained from the supplementary methodologies.

For data analysis, we utilized the "TwoSampleMR" package for the analysis, while the "tidyverse," "data. table," and "R.utils" packages facilitated data processing. The "ggplot2" package was employed for data visualization. Finally, we used Adobe Illustrator to arrange and number the visualizations generated in the R language.[36] We implemented a Benjamini–Hochberg false discovery rate (FDR) correction to adjust for multiple comparisons involving four exposures. The FDR, defined as the anticipated proportion of findings that are erroneously rejected, has been recently introduced as an alternative statistic for controlling multiple testing. The FDR demonstrates superior efficacy in identifying true positives while maintaining the fraction of type I errors at a predetermined threshold.[37] P values below 0.05 that did not survive the FDR adjustment were deemed indicative of a possible connection. Analyses were executed utilizing R version 4.5.0, with the MR analysis carried out via the “TwoSampleMR” package version 0.6.15.

3.1. Statistical analysis

A complete sensitivity analysis was undertaken to determine the trustworthiness of our findings and to reduce potential biases from heterogeneity and pleiotropy. The Cochran Q-test was used to assess the homogeneity among the SNPs, with a p-value over 0.05 indicating a lack of heterogeneity. The intersection of the MR-Egger and IVW techniques was analyzed for pleiotropy assessment; a p-value beyond 0.05 signified the lack of horizontal pleiotropy. The MR Polygenic Risk Score Summarization-Outlier (MR-PRESSO) test was utilized to identify outlier SNPs affected by horizontal pleiotropy, with a p-value above 0.05 in the Global test indicating the existence of these outliers.[38] Considering that SNPs may influence exposure through outcomes, resulting in inaccurate causal conclusions, especially in complex biological interactions, the Steiger test was conducted to ascertain the directionality of the link among the proteome, metabolome, and LDH.

Simultaneously, we employed the TwoSampleMR package to generate funnel plots and leave-one-out plots of the SNP distributions in the MR analyses, which were utilized to evaluate the robustness of the MR analyses' conclusions.[39,40]

3.2. Functional annotation and pathway enrichment analysis

In order to identify the proteins that are involved in the causal relationship between proteins and LDH, we conducted functional annotation to determine their biological significance. Utilizing the R packages "clusterProfiler" and "org.Hs.eg.db," pathway enrichment studies were conducted to identify pathways that were enriched with the identified proteins in the Gene Ontology (GO) and Kyoto Encyclopedia of Genes and Genomes (KEGG). Furthermore, we developed a Protein-Protein Interaction (PPI) network utilizing data from the GENEMANIA database. Finally, we utilized Cytoscape software to investigate the putative pathways involving the identified proteins and metabolites.

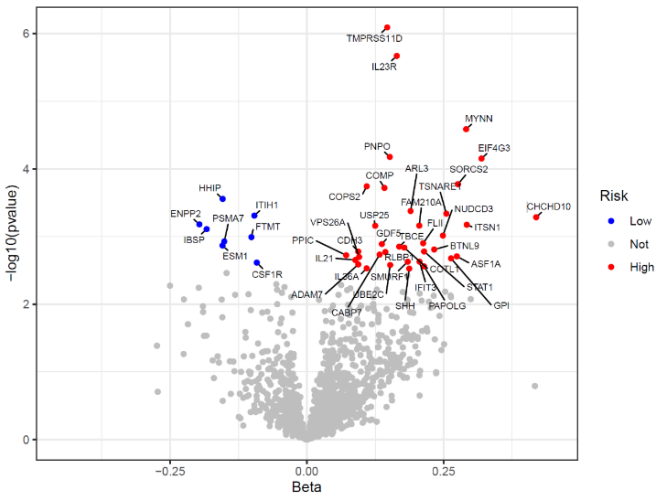

Figure 2: Differential expression of plasma proteins associated with LDH. Blue represents downregulated genes, while red represents upregulated genes.

ISSN 2618-1584 Vol. 7, Issue 6: 125-140, DOI: 10.25236/FMSR.2025.070616

4. Results

4.1. MR analysis of plasma proteome and LDH

Following the screening of IVs, we identified a total of 31,315 SNPs associated with cis-pQTLs in the plasma proteome. All identified IVs demonstrated robustness, with F-values exceeding 29.7, derived from 3,595 proteins. We employed the IVW method as an absolute evaluation metric. The proteins with consistent OR values from the five methods were extracted, and the multi-effect results were excluded, using the filtering criteria of IVW-pvalue < 0.005 and FDR < 0.2. The OR value greater than 1 indicates that the exposure is a risk factor for the outcome, while the OR value less than 1 suggests that the exposure serves as a protective factor. Ultimately, 44 significant proteins were screened for a causal association with LDH. Fig.2 shows that, after p-value adjustment, 36 proteins, including PAPOLG (p value=2.76E-03, FDR=0.19, OR=1.24, 95%CI=1.08-1.43), remained associated with LDH as a risk factor, and 8 proteins, including ENPP2 (p value=6.60E-04, FDR=0.13, OR=0.82, 95%CI=0.73-0.92), were associated with LDH as a protective factor. A volcano plot in Fig.2 visually displays the association of the 44 proteins with LDH risk, coded by blue for protective effects and red for risk factors. The SNPs are uniformly distributed on either side of the funnel plot, whereas the leave-one-out method points are predominantly located on one side, reinforcing the robustness of the findings. The directionality assessment verified that all 44 proteins (as shown in Fig.3) identified through analysis had the expected causal relationship with LDH. The results of the heterogeneity and pleiotropy assessments revealed no heterogeneity or pleiotropy within the dataset, except for the identified heterogeneity in CSF1R, ITIH1, and FTMT. Notably, although a certain degree of heterogeneity was observed in our analysis, the use of a random-effects model (IVW) effectively mitigated its impact on the overall results. Consequently, our conclusions remain primarily based on the IVW method, which demonstrated a significant association between these genetic instruments and the exposure or outcome variable. Using FTMT as an example, inspection of the forest plot (Fig.4A) clearly demonstrates that the confidence intervals for the majority of individual SNPs do not encompass zero, thereby indicating that their effects are statistically significant. The results from both the MR Egger and IVW analyses indicated no evidence of significant horizontal pleiotropy. Fig.4B illustrates the leave-one-out sensitivity analysis, which involved iteratively excluding each SNP to evaluate whether the overall causal estimate was unduly influenced by any single genetic variant. In this plot, the central overall effect estimate is represented by the red dot, with its corresponding confidence interval indicated by the horizontal line. The plot shows little change in the effect estimates upon the removal of each SNP, with all values remaining on the left of zero, indicating that no individual variant significantly altered the overall results and attesting to the stability of the MR effect. The Funnel Plot (Fig.4C) is a graphical tool primarily used to assess the presence of pleiotropy, a potential source of bias in MR studies. The overall symmetry of the funnel plot, with no significant skewness or outlier aggregation, suggests there is no compelling evidence for horizontal pleiotropy or selection bias that would invalidate the causal inference. The consistent effect estimates observed between the MR Egger and IVW methods further strengthen the evidence for a robust and reliable causal effect. This scatter plot depicts the bivariate relationships between the exposure and outcome effect estimates for all instrumental variables. Herein, the fitted lines, differentiated by color, correspond to the aggregated causal effect estimates generated by various MR methods, including IVW, MR Egger, and weighted median. Observed in Fig.4D, the majority of data points fall below zero with a relatively concentrated distribution, a pattern notably suggestive of specific SNP effects. Consistently negative slopes across the various MR methods provide robust evidence supporting a significant causal effect of FTMT on LDH. Furthermore, the observed concordance in the directional estimates attests to the robustness of the underlying MR analysis.

ISSN 2618-1584 Vol. 7, Issue 6: 125-140, DOI: 10.25236/FMSR.2025.070616

exposure	nsnp	method	pval	OR(95% CI)
ADAM7	3	Weighted median	0.005	1.096 (1.028 to 1.168)
	3	Inverse variance weighted	0.003	1.098 (1.033 to 1.168)
ARL3	3	Weighted median	0.002	1.201 (1.070 to 1.348)
	3	Inverse variance weighted	<0.001	1.209 (1.088 to 1.343)
ASF1A	4	Weighted median	0.003	1.365 (1.114 to 1.671)
	4	Inverse variance weighted	0.002	1.315 (1.106 to 1.564)
BTNL9	3	Weighted median	0.017	1.229 (1.037 to 1.455)
	3	Inverse variance weighted	0.002	1.262 (1.093 to 1.457)
CABP7	7	Weighted median	0.034	1.125 (1.009 to 1.254)
	7	Inverse variance weighted	0.002	1.142 (1.050 to 1.242)
CDH3	12	Weighted median	0.002	1.095 (1.033 to 1.162)
	12	Inverse variance weighted	0.002	1.098 (1.036 to 1.164)
CHCHD10	3	Weighted median	<0.001	1.602 (1.304 to 1.968)
	3	Inverse variance weighted	<0.001	1.521 (1.200 to 1.926)
COMP	11	Weighted median	<0.001	1.194 (1.104 to 1.291)
	11	Inverse variance weighted	<0.001	1.152 (1.070 to 1.241)
COPS2	8	Weighted median	<0.001	1.113 (1.047 to 1.184)
	8	Inverse variance weighted	<0.001	1.115 (1.053 to 1.181)
COTL1	5	Weighted median	0.017	1.153 (1.026 to 1.296)
	5	Inverse variance weighted	0.001	1.195 (1.071 to 1.333)
CSF1R	23	Weighted median	0.175	0.957 (0.898 to 1.020)
	23	Inverse variance weighted	0.002	0.912 (0.860 to 0.968)
EIF4G3	3	Weighted median	<0.001	1.381 (1.163 to 1.640)
	3	Inverse variance weighted	<0.001	1.376 (1.175 to 1.610)
ENPP2	5	Weighted median	<0.001	0.780 (0.676 to 0.901)
	5	Inverse variance weighted	<0.001	0.822 (0.734 to 0.920)
ESM1	8	Weighted median	0.018	0.886 (0.801 to 0.980)
	8	Inverse variance weighted	0.001	0.857 (0.780 to 0.942)
FAM210A	4	Weighted median	<0.001	1.303 (1.133 to 1.498)
	4	Inverse variance weighted	<0.001	1.228 (1.091 to 1.383)
FLII	3	Weighted median	0.004	1.235 (1.068 to 1.429)
	3	Inverse variance weighted	0.001	1.237 (1.087 to 1.407)
FTMT	11	Weighted median	<0.001	0.878 (0.829 to 0.931)
	11	Inverse variance weighted	0.001	0.904 (0.850 to 0.960)
GDF5	4	Weighted median	0.002	1.154 (1.054 to 1.263)
	4	Inverse variance weighted	0.001	1.147 (1.055 to 1.246)
GPI	4	Weighted median	0.030	1.254 (1.022 to 1.539)
	4	Inverse variance weighted	0.002	1.301 (1.100 to 1.539)
HHIP	7	Weighted median	0.005	0.867 (0.785 to 0.958)
	7	Inverse variance weighted	<0.001	0.857 (0.789 to 0.932)
IBSP	8	Weighted median	0.006	0.843 (0.746 to 0.953)
	8	Inverse variance weighted	<0.001	0.833 (0.748 to 0.926)
IFIT3	3	Weighted median	0.006	1.234 (1.062 to 1.435)
	3	Inverse variance weighted	0.002	1.229 (1.076 to 1.403)
IL21	7	Weighted median	0.006	1.093 (1.026 to 1.165)
	7	Inverse variance weighted	0.002	1.092 (1.032 to 1.156)
IL23R	4	Weighted median	<0.001	1.176 (1.094 to 1.264)
	4	Inverse variance weighted	<0.001	1.179 (1.101 to 1.261)
IL36A	4	Weighted median	0.020	1.095 (1.014 to 1.183)
	4	Inverse variance weighted	0.003	1.115 (1.038 to 1.198)
ITIH1	15	Weighted median	<0.001	0.881 (0.834 to 0.931)
	15	Inverse variance weighted	<0.001	0.908 (0.861 to 0.959)
ITSN1	3	Weighted median	0.004	1.322 (1.094 to 1.598)
	3	Inverse variance weighted	<0.001	1.339 (1.132 to 1.585)
MYNN	4	Weighted median	<0.001	1.321 (1.120 to 1.557)
	4	Inverse variance weighted	<0.001	1.338 (1.168 to 1.532)
NUDCD3	3	Weighted median	0.004	1.298 (1.089 to 1.546)
	3	Inverse variance weighted	<0.001	1.282 (1.106 to 1.486)
PAPOLG	3	Weighted median	0.016	1.217 (1.037 to 1.427)
	3	Inverse variance weighted	0.003	1.239 (1.077 to 1.425)
PNPO	4	Weighted median	<0.001	1.169 (1.071 to 1.276)
	4	Inverse variance weighted	<0.001	1.164 (1.080 to 1.253)
PPIC	13	Weighted median	0.739	1.011 (0.947 to 1.080)
	13	Inverse variance weighted	0.002	1.074 (1.027 to 1.124)
PSMA7	6	Weighted median	0.137	0.913 (0.809 to 1.029)
	6	Inverse variance weighted	0.001	0.860 (0.785 to 0.942)
RLBP1	3	Weighted median	0.002	1.157 (1.054 to 1.270)
	3	Inverse variance weighted	0.002	1.154 (1.055 to 1.262)
SHH	4	Weighted median	0.025	1.183 (1.022 to 1.369)
	4	Inverse variance weighted	0.003	1.206 (1.066 to 1.364)
SMURF1	3	Weighted median	0.003	1.219 (1.069 to 1.390)
	3	Inverse variance weighted	0.002	1.202 (1.068 to 1.354)
SORCS2	4	Weighted median	0.001	1.306 (1.110 to 1.535)
	4	Inverse variance weighted	<0.001	1.318 (1.141 to 1.522)
STAT1	4	Weighted median	0.015	1.229 (1.041 to 1.450)
	4	Inverse variance weighted	0.002	1.239 (1.084 to 1.416)
TBCE	6	Weighted median	0.009	1.179 (1.042 to 1.335)
	6	Inverse variance weighted	0.001	1.184 (1.067 to 1.313)
TMPRSS11D	8	Weighted median	<0.001	1.165 (1.094 to 1.241)
	8	Inverse variance weighted	<0.001	1.158 (1.092 to 1.228)
TSNARE1	3	Weighted median	0.007	1.234 (1.059 to 1.438)
	3	Inverse variance weighted	<0.001	1.290 (1.119 to 1.488)
UBE2C	3	Weighted median	0.009	1.152 (1.036 to 1.281)
	3	Inverse variance weighted	0.003	1.164 (1.054 to 1.286)
USP25	8	Weighted median	0.023	1.103 (1.014 to 1.201)
	8	Inverse variance weighted	<0.001	1.133 (1.054 to 1.218)
VPS26A	9	Weighted median	0.013	1.096 (1.019 to 1.179)
	9	Inverse variance weighted	0.002	1.100 (1.035 to 1.169)

Figure 3: Causal effect of Plasma protein-regulated gene on LDH. OR Odds Ratio; CI Confidence Interval.

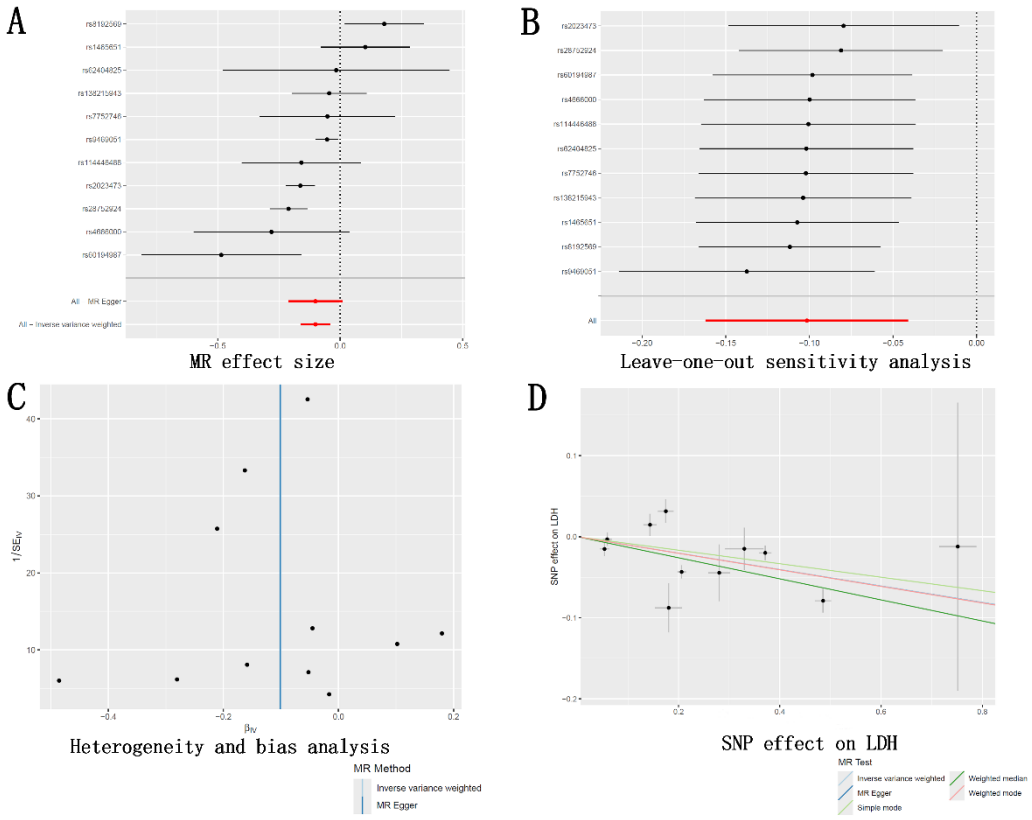

Figure 4: Causal Effects of LDH on FTMT. (A. Forest Plot B. leave-one-out Plot C. funnel plot D. scatter Plot).

ISSN 2618-1584 Vol. 7, Issue 6: 125-140, DOI: 10.25236/FMSR.2025.070616

4.2. Reverse MR analysis of plasma proteome and LDH

Figure 3 illustrates the causative relationship between the plasma proteome and LDH; this section will examine the inverse relationship between the plasma proteome and LDH. We performed a study on the 44 proteins utilizing the LDH previously reported as having substantial causal connections. The GWAS data of LDH were examined independently using the aforementioned approach, with a p-value threshold of less than 5e-8. Subsequently, linkage disequilibrium was eliminated. The collected data were filtered based on F > 10 to exclude weak instrumental variables; ultimately, we identified 30 SNPs as instrumental variables. The MR analysis, heterogeneity, and pleiotropy assessments were performed on the 30 SNPs instrumental variables and the GWAS data for 44 protein types acquired. Following the removal of proteins PNPO and COTL1 due to pleiotropy identified in the pleiotropy and heterogeneity tests, the IVW results suggest revealed that FAM210A, PSMA7, RLBP1, SMURF1, UBE2C, COPS2, and MYNN may be consequences of LDH(OR: 0.923, 95%CI: 0.871-0.978, P=0.007; OR: 0.931, 95%CI: 0.871-0.995, P=0.035; OR: 0.912, 95%CI: 0.860-0.967, P=0.002; OR: 0.928, 95%CI: 0.876-0.982, P=0.010; OR: 0.934, 95%CI: 0.883-0.989, P=0.018; OR: 0.939, 95%CI: 0.886-0.995, P=0.033; OR: 0.943, 95%CI: 0.891-0.998, P=0.029). Subsequently, we conducted tests for pleiotropy and heterogeneity on the obtained data. The leave-one-out analysis validated the robustness of our MR analysis, since it remained unaffected by any particular SNP.

4.3. MR analysis of plasma metabolome and LDH

By setting the p-value threshold to 1×10^{-5} and removing linkage disequilibrium, our instrumental variable selection identified 34,843 genetic instrument SNPs, with a minimum F-statistic exceeding 19. By establishing a filtering criterion of IVW-pvalue < 0.01, we identified metabolites with consistent odds ratios across the five methodologies and eliminated multiple-effect outcomes. Subsequently, we evaluated 23 metabolites for significant causal relationships from 1400 metabolite profiles that were amenable to causal analysis, which are shown in Figure 5 The outcomes of the heterogeneity and pleiotropy analyses indicated the presence of heterogeneity among the N6-methyllysine levels, Inosine 5'-monophosphate (IMP) to phosphate ratio, and Octadecenedioate (C18:1-DC) levels. Consistent with the previous approach, these results were included in the subsequent analysis, given that the application of a random-effects model, which was predominantly used in this study, effectively minimized the impact of heterogeneity on the overall results. Egger's intercept revealed an absence of pleiotropy across all tested variables. Similarly, the leave-one-out analysis provided evidence for the reliability of the Mendelian randomization results.

exposure	nsnp	method	pval	OR(95% CI)
2−hydroxy−3−methylvalerate levels	30	Inverse variance weighted	0.004	1.061 (1.019 to 1.104)
2−methylserine levels	26	Inverse variance weighted	0.003	1.024 (1.008 to 1.039)
3−hydroxydecanoylcarnitine levels	29	Inverse variance weighted	<0.001	0.933 (0.898 to 0.969)
4−methoxyphenol sulfate levels	20	Inverse variance weighted	0.001	1.084 (1.032 to 1.138)
Alpha−ketoglutarate to kynurenine ratio	26	Inverse variance weighted	0.004	1.053 (1.016 to 1.092)
Carnitine C5:1 levels	26	Inverse variance weighted	0.004	0.941 (0.903 to 0.980)
Cholesterol to cortisol ratio	17	Inverse variance weighted	0.002	0.916 (0.867 to 0.967)
Cortisol levels (plasma)	20	Inverse variance weighted	0.006	1.082 (1.023 to 1.144)
Cysteine to 5−oxoproline ratio	19	Inverse variance weighted	0.008	1.050 (1.013 to 1.088)
Histidine levels	22	Inverse variance weighted	0.003	0.947 (0.914 to 0.981)
Inosine 5'−monophosphate (IMP) to phosphate ratio	20	Inverse variance weighted	0.004	1.071 (1.022 to 1.121)
N−acetyl−L−glutamine levels	23	Inverse variance weighted	0.009	0.969 (0.946 to 0.992)
N2−acetyl,N6−methyllysine levels	29	Inverse variance weighted	0.006	0.983 (0.971 to 0.995)
N6−methyllysine levels	33	Inverse variance weighted	0.008	0.966 (0.942 to 0.991)
Octadecadienedioate (C18:2−DC) levels	32	Inverse variance weighted	0.003	0.960 (0.935 to 0.986)
Octadecenedioate (C18:1−DC) levels	22	Inverse variance weighted	0.002	0.943 (0.909 to 0.979)
Phosphocholine levels	35	Inverse variance weighted	0.004	1.035 (1.011 to 1.060)
Pyruvate levels	22	Inverse variance weighted	0.008	0.930 (0.882 to 0.982)
Thioproline levels	25	Inverse variance weighted	0.004	1.065 (1.021 to 1.110)
X−13553 levels	25	Inverse variance weighted	0.004	1.060 (1.018 to 1.104)
X−15461 levels	24	Inverse variance weighted	<0.001	1.086 (1.039 to 1.135)
X−21319 levels	14	Inverse variance weighted	0.005	1.083 (1.024 to 1.145)
X−24307 levels	16	Inverse variance weighted	<0.001	0.889 (0.838 to 0.942)

Figure 5: Causal effect of Plasma metabolite-regulated gene on LDH. OR Odds Ratio; CI Confidence Interval.

ISSN 2618-1584 Vol. 7, Issue 6: 125-140, DOI: 10.25236/FMSR.2025.070616

4.4. PPI and enriched pathways of the proteins

Utilizing the GeneMANIA database, we established a PPI network to investigate the functionality of these proteins (Fig.6). The interactions between these MR-identified proteins, which contained 44 nodes, are depicted in the PPI network plot. Then, using the clusterProfiler R package, we conducted GO analysis on the positive plasma protein genes identified in the forward MR investigation. The results indicated that a total of 9 CC, 29 MF, and 316 BP terms were significantly enriched, with all differences exhibiting statistical significance ($P < 0.05$). Figure 7A presents an annular chart that encapsulates the findings of the GO study of positively identified plasma protein genes from forward MR investigations. The illustration has four circular rings: the outermost layer displays the 18 most enriched categories from the GO analysis. Various hues denote the GO categories: purple for Molecular Function (MF), yellow for Cellular Component (CC), and green for Biological Process (BP). The second ring denotes the entire gene count inside the genomic context, along with the Q values of up-regulated genes associated with a certain biological event. Significantly, GO: 0062023 (extracellular matrix containing collagen) exhibited the largest gene count (432) and demonstrated the greatest enrichment. The third ring illustrates the quantity of differential genes inside every enrichment pathway. The picture illustrates that the cytokine receptor binding in MF exhibits the greatest gene counts, underscoring their significant importance in LDH pathogenesis. The last ring illustrates the enrichment factor for every GO. The concentrations of GO: 0072203 (cell proliferation involved in metanephros development) and GO: 2001054 (negative regulation of mesenchymal cell apoptotic process) were the highest, suggesting the potential mechanisms of LDH involving cellular proliferation and inflammatory-immune responses. Figure 7B illustrates the top 10 biological processes in the Gene Ontology analysis, determined by the lowest P values. The first two components of the CC are the collagen-containing extracellular matrix and the ciliary membrane. The top five MF are cytokine receptor binding, cytokine binding, growth factor receptor binding, cytokine activity, and ubiquitin-like protein ligase binding. The top three BP are cell surface receptor signaling pathway via JAK−STAT, cell surface receptor signaling pathway via STAT, and positive regulation of leukocyte proliferation. Utilizing KEGG Pathway analysis, we discovered nine signal transduction pathways ($P < 0.05$) (Fig.7C). The top signaling pathway is the Cytokine-Cytokine receptor interaction. These pathways are crucial to the disease's genesis and progression, as they collectively regulate inflammatory responses, signal transmission, metabolic processes, and cell proliferation and apoptosis.

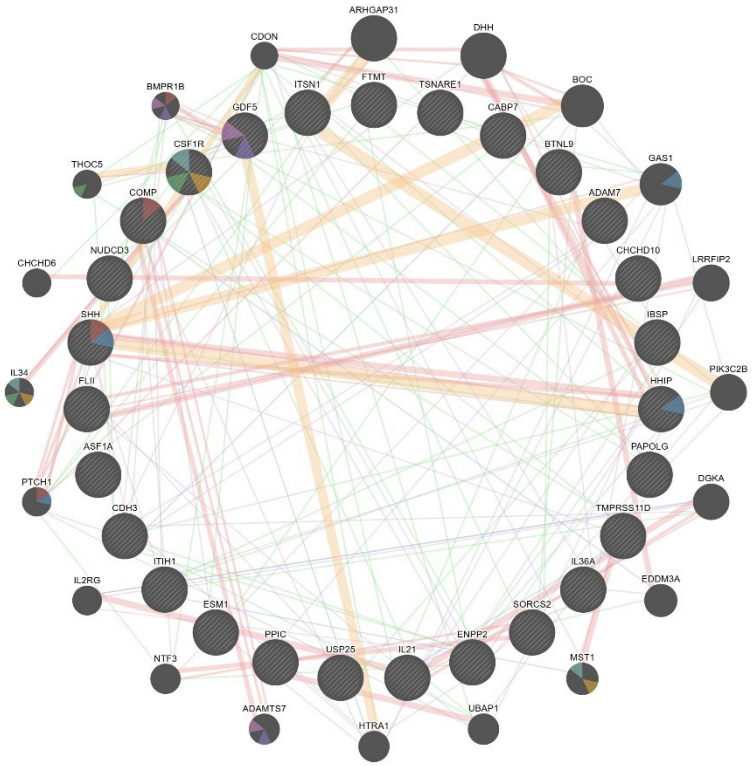

Figure 6: Protein-protein interaction network.

ISSN 2618-1584 Vol. 7, Issue 6: 125-140, DOI: 10.25236/FMSR.2025.070616

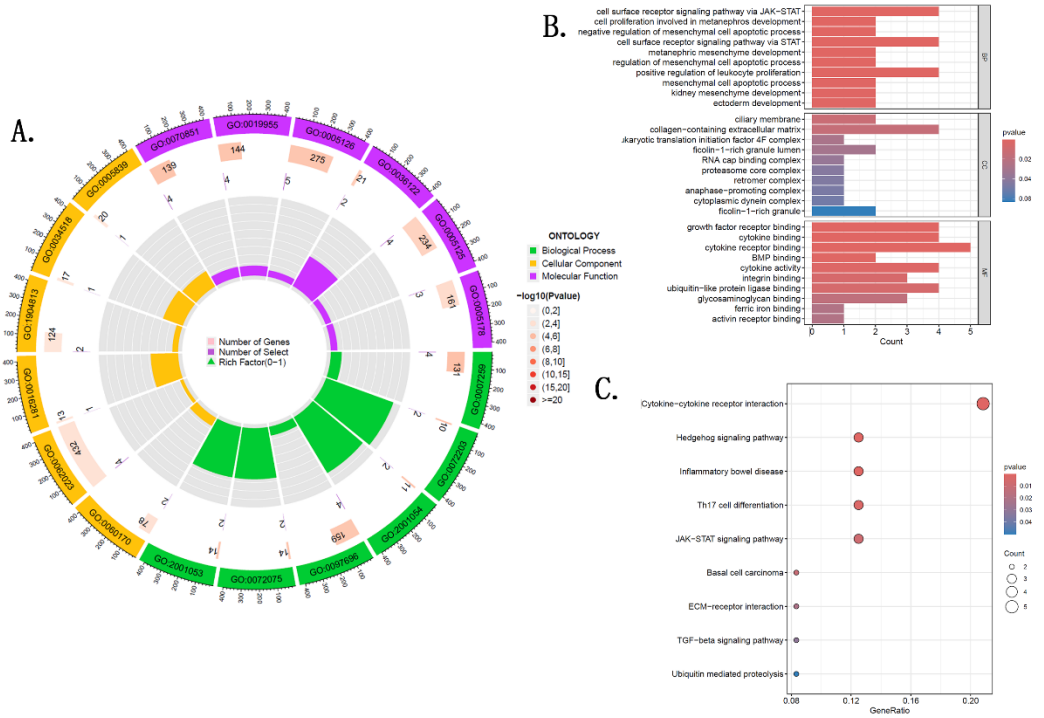

Figure 7: GO and KEGG enrichment of plasma protein genes (A. The cycle diagram of GO enrichment, B. the barplot of GO enrichment, C. the bubble diagram of KEGG enrichment).

5. Discussion

This study performed the first Mendelian randomization (MR) analysis of the plasma proteome and metabolome in relation to lumbar disc herniation (LDH) using European GWAS data. We identified potential protein targets and employed linkage disequilibrium removal and pleiotropy testing to minimize confounding bias.

Proteomic MR analysis identified 44 protein markers: genetically predicted levels of 36 circulating proteins (e.g., CHCHD10, STAT1, IL23R) were associated with increased LDH risk, while 8 proteins (e.g., PSMA7, HHIP, ENPP2) were associated with decreased risk. Reverse MR suggested nine proteins, including FAM210A and PSMA7, might be consequences of LDH, with COTL1 and PNPO showing pleiotropy. PPI network and enrichment analyses indicated these proteins are primarily involved in immune responses.

Metabolomic MR analysis identified 23 significant circulating metabolites. Subsequently, using the Cytoscape 3.10.3 software, pathway analysis was performed on the identified metabolites and target proteins to elucidate potential relevant pathways. Construction using the Metscape plugin within Cytoscape suggested four potential metabolic pathways: the ENPP2-Cystine pathway involved in the vitamin B5-CoA biosynthesis from panthenate (Fig.8A); the ENPP2-NAG (N-acetyl-L-glutamine) pathway participating in vitamin B3 (niacin and nicotinamide) metabolism (Fig.8B); the FTMT-Cystine pathway implicated in the metabolism of methionine and cysteine (Fig.8C); and the PAPOLG-IMP pathway associated with purine metabolism (Fig.8D).

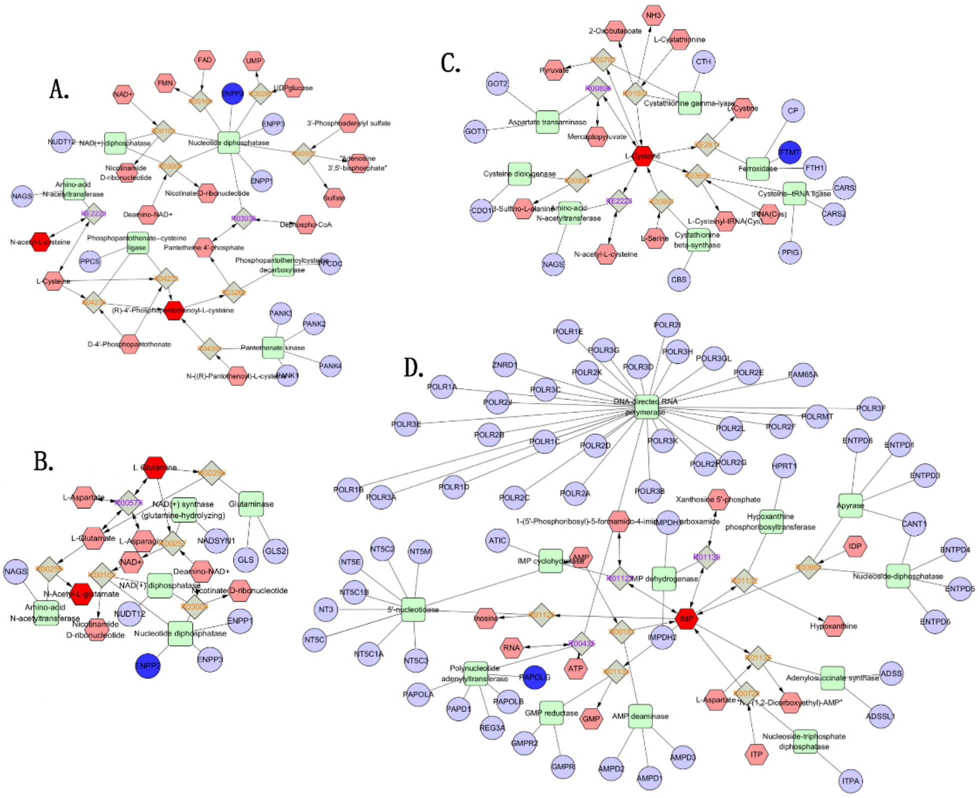

Figure 8: The metabolic pathways constructed by Cytoscape (A. The ENPP2-Cystine pathway; B. the ENPP2-NAG pathway; C. the FTMT-Cystine pathway; D. the PAPOLG-IMP pathway).

Autotaxin (ATX) is encoded by the ENPP2 gene in the human chromosomal region 8q24 and is a 125-kD-secreted glycoprotein. ENPP2/Autotaxin is widely present in biological fluids, including blood, with pyrophosphatase/phosphodiesterase activities and lysophospholipase D activity.[41] Lysophosphatidic acid (LPA) is produced from lysophosphatidylcholines (LPC) through the action of the enzyme ATX.[42] Furthermore, ATX is proposed to interact with integrins on the cell surface, so evading clearance and potentially guiding LPA to neighboring receptors, thereby localizing the actions of LPA.[43–45] The ATX/LPA axis has demonstrated significant involvement in various pathological processes, particularly relevant to chronic inflammation, including chronic neuropathic pain.[46] Human correlational data, along with genetic and pharmacological research in mice and numerous in vitro investigations, indicate that ATX and LPA signaling are significant contributors to chronic inflammation and potential therapeutic targets in various disorders.[41] An analysis of LPA levels in female patients with fibromyalgia and other pain conditions revealed that the LDH group exhibited significantly higher LPA levels compared to the degenerative disc disease group (p = 0.04), but showed no significant difference when compared to the healthy control group (p = 0.8).[47] In both our MR and reverse MR analyses, ENPP2 (OR: 0.821, 95%CI: 0.734-0.920, P=6.6E-04) was found to be a protective factor for LDH, and there was no reverse causal relationship between ENPP2 and LDH, which aligns with the findings of the previously cited study.

The TSMR analysis conducted later regarding plasma circulating metabolites and LDH revealed a theoretical causal relationship between the ratio of cysteine and 5-oxoproline and LDH (GCST90200785, OR: 1.050, 95%CI: 1.013-1.088, P=8.2E-03), which indicates that the cysteine to 50oxoproline ratio is a theoretical risk factor for LDH. The relationship between the ratio and LDH has not been reported by any relevant studies yet. But as an endogenous cysteine metabolite, N-Acetyl-L-cysteine (NAC) has demonstrated analgesic effects in both inflammatory pain models and in a neuropathic pain model induced by chronic constriction injury.[48] A randomized controlled clinical trial demonstrated that NAC, when used as an adjunct to NSAIDs, may alleviate pain and enhance pain-related impairment in individuals with acute lumbar radiculopathy due to disc herniation.[49] Moreover, numerous studies have substantiated that reactive oxygen species (ROS) facilitate matrix breakdown and inflammation, resulting in an increase in senescent cells and a decrease in viable cells within the intervertebral disc milieu, hence exacerbating disc degeneration. ROS are highly reactive oxygen-containing molecules that encompass:

ISSN 2618-1584 Vol. 7, Issue 6: 125-140, DOI: 10.25236/FMSR.2025.070616

hydrogen peroxide (H_2O_2), singlet oxygen ($^1O_2$), superoxide anion ($O_2•^-$), and hydroxyl radical (•OH). Their primary functions are to regulate cell matrix metabolism, inflammation, apoptosis, autophagy, and aging.[50] Recent reports indicate that NAC, as an antioxidant, significantly contributes to the postponement of intervertebral disc degeneration, a primary factor in LDH. A study including animal experimentation has demonstrated that NAC mitigates the catabolism of reactive oxygen species (ROS) during intervertebral disc degeneration in rats, thereby preventing the denaturation of the intervertebral disc.[51] Meanwhile, in vivo studies of imaging and tissue morphology indicated that the disc height index, magnetic resonance imaging grade, and histology score considerably improved compared to degenerative models following the application of N-acetylcysteine-derived carbon dots.[52] When conducting the integrated analysis of proteomics and metabolomics using Cytoscape, we identified this possible metabolic pathway involving ENPP2 and cysteine, which reveals how they interact with each other to contribute to LDH. As the reduction of Cysteine occurs through its conversion into N-Acetyl-L-cysteine and Pantetheine 4'-phosphate via distinct metabolic pathways, N-Acetyl-L-cysteine reduces the risk of intervertebral disc degeneration by acting as an antioxidant. Concurrently, Pantetheine 4'-phosphate—a metabolite of ENPP2—inhibits the R03036 pathway, thereby increasing ENPP2, which serves as a protective factor for LDH (Fig.8A).

Acetylglutamine (N-acetyl-L-glutamine, NAG), produced via the acetylation of glutamine, functions as a metabolic precursor that can be degraded into two principal metabolites: glutamic acid (Glu) and γ-aminobutyric acid (GABA).[53] GABA has the capacity to maintain the brain's normal function and increase the activity of acetylcholine.[54] Furthermore, Glu serves as an excitatory neurotransmitter that is closely linked to neural plasticity and is essential in processes such as neuronal growth and synaptogenesis.[55] Growing data suggest that NAG has a crucial neuroprotective role against cerebral ischemia-reperfusion injury by decreasing neuronal death and inflammation.[53] In addition, Guhong Injection (GHI), mostly composed of NAG and safflower extract, has demonstrated efficacy in augmenting fracture healing through the stimulation of osteoblast differentiation and proliferation, along with the activation of the Wnt/beta-catenin signaling pathway by GHI.[56] Experimental evidence from a rat model demonstrates that NAG suppresses inflammatory responses and improves the survival of motor neurons[57], suggesting a potential mechanism for its protective effects in LDH(OR: 0.969, 95%CI: 0.946-0.992, P=9.33E-03). As illustrated in Figure 8B, the network constructed using Cytoscape reveals that N-acetyl-L-glutamine (NAG) participates in vitamin B3 metabolism in conjunction with ENPP2 through its conversion to glutamine, thereby collectively exerting protective effects against LDH. However, the precise underlying mechanism of action requires further investigation to be fully elucidated.

The mitochondrial ferritin (FTMT) was recognized about 20 years ago as a particular protein responsible for iron deposition in mitochondria.[58] The human FTMT gene is located on chromosome 5q23.1 and encodes a precursor of a ferritin H-like protein consisting of 242 amino acids. The principal role of FTMT is not the storage of cellular iron, but rather the protection of mitochondria from iron-dependent oxidative damage.[59] The overexpression of FTMT has been demonstrated to facilitate the translocation of iron from the cytosol to the mitochondria.[60] The mitochondrial location of FTMT aligns with its principal role of regulating ROS production via managing mitochondrial iron supply.[61] In other words, FTMT reduced the level of ROS and had a positive effect on cell viability, thereby inhibiting the role of ROS in aggravating intervertebral disc degeneration. Corroborating the above findings, our MR and reverse MR analyses indicate that FTMT is a putative protective factor (OR: 0.904, 95%CI: 0.850-0.960, P=1.02E-03) for LDH without reverse causation. Similarly, Figure 8C illustrates the potential metabolic pathway through which Cysteine and FTMT jointly act on LDH.

Poly(A) polymerase gamma (PAPOLG), a constituent of the poly(A) polymerase (PAP) family, is crucial for mRNA stability and translational alterations.[62] The poly(A) tail is essential for mRNA stability, as it assists in mRNA transport to the cytoplasm and promotes efficient translation.[63] A separate investigation demonstrated that PAPOLG modulates NF-κB expression and fosters a prolonged inflammatory response, which is characterized by elevated levels of IL-6 and TNF-α. Thus, pharmacological treatments or small compounds that inhibit PAPOLG may alleviate excessive inflammatory reactions.[64] In our proteome-wide MR analysis for LDH, PAPOLG was revealed as a risk factor and potential therapeutic target (OR: 1.239, 95%CI:1.077- 1.425, P=2.76E-03). To date, no studies have clearly confirmed how PAPOLG influences LDH. Considering the pathological processes underlying LDH and the biochemical action of PAPOLG, we reasonably infer that this is related to PAPOLG's promotion of inflammatory responses. The identification of PAPOLG as a therapeutic target presents a novel conceptual approach for the treatment of LDH, though this proposition warrants further investigation to validate its clinical applicability.

Inosine 5′-monophosphate (5′-IMP) is a crucial nucleotide for de novo nucleotide production and the

ISSN 2618-1584 Vol. 7, Issue 6: 125-140, DOI: 10.25236/FMSR.2025.070616

metabolism of energy and proteins.[65] It can also allow animals to detect novel flavors.[66] Zhang et al. discovered that the oral administration of IMP to mice facilitated the uptake of exogenous fatty acids and their conversion to triglycerides, while also augmenting the phosphorylation of liver IMP-activated protein kinase, leading to hyperplasia of adipose tissue.[67] A separate study revealed the role of IMP metabolism in regulating UCP-1 expression and adipocyte growth, offering new insights that indicate IMP metabolism as a viable therapeutic target for obesity treatment.[68] Obesity and excess weight are risk factors for lumbar radiculopathy and sciatica in both genders, exhibiting a dose-response connection, as indicated by a meta-analysis encompassing data from 26 clinical studies. Similarly, analogous results were derived from a recent meta-analysis encompassing ten cohort studies.[69] This is consistent with our results, which demonstrate IMP as a risk factor contributing to LDH. Nevertheless, it is important to acknowledge that certain heterogeneity was observed within our analytical findings; however, its influence on the overall findings was negligible. Similarly, Figure 8D of purine metabolism delineates the putative metabolic pathway through which PAPOLG and IMP cooperatively influence LDH, though this mechanistic model requires experimental validation to confirm its biological relevance.

In this study, employing multivariate MR for a comprehensive exploration of the associations among circulating plasma proteins, metabolites, and LDH risk provided several key advantages. TS MR provides significant advantages owing to its comprehensive proteome coverage, large sample size, and reduced confounding bias and possibility of reverse causality. The robustness of our findings was supported by a comprehensive analytical framework that included evaluations for validity, sensitivity, and pleiotropy. Furthermore, the integration of metabolomics and proteomics data yielded significant insights into the pathological mechanisms of LDH from a metabolic pathway viewpoint, which contributes to pinpointing potential therapeutic targets. The originality of the current study resides in the amalgamation of two-sample MR analysis with multi-omics analysis, offering a distinctive analytical framework for determining causal correlations among circulating plasma proteins, plasma metabolites, and LDH. A key distinction of our study lies in this dual approach, which facilitates a more accurate pinpointing of protein biomarkers and therapeutic targets, contrasting with previous studies that were mainly dependent on observational data. This establishes a new paradigm for the future discovery of biomarkers and identification of therapeutic targets for LDH and other complex diseases. Nevertheless, specific limits must be recognized. Firstly, our MR findings, derived from whole-blood circulating proteins and metabolites, necessitate validation through in vivo and in vitro research, together with randomized controlled trials (RCTs), to furnish more direct proof substantiating our claims. Secondly, as our study focused exclusively on individuals of European ancestry, validation in diverse populations is essential prior to any generalization of the findings. The interplay between genetic factors and environmental influences may constrain the applicability of our results.

6. Conclusions

Through MR analysis, we identified 44 plasma proteins and 23 plasma metabolites significantly associated with LDH. To further interpret these findings, we employed an integrated bioinformatic approach including PPI network construction, GO enrichment, and KEGG pathway analyses. These investigations revealed that the identified proteins not only engage in functional interactions but are also enriched in pathways related to inflammatory response, signal transduction, and cytokine-cytokine interactions. Additionally, using Cytoscape software, we mapped potential theoretical metabolic pathways involving specific molecular pairs such as ENPP2 and cysteine, ENPP2 and NAG, FTMT and cysteine, and PAPOLG and IMP. Consequently, we identified three potential therapeutic targets for LDH: ENPP2, FTMT, and PAPOLG. While these results suggest plausible biological mechanisms, the functional interactions among these molecules require further experimental validation.

Ethics Approval

The GWAS datasets included in this research were obtained from publicly accessible, ethically approved studies, eliminating the necessity for new sample collection and additional ethical approval for this investigation. The ethical declaration in our research is inapplicable.

Author contributions

All authors have designed the study, developed the methodology, and written the manuscript. All authors have read and agreed to the published version of the manuscript.

ISSN 2618-1584 Vol. 7, Issue 6: 125-140, DOI: 10.25236/FMSR.2025.070616

Acknowledgments

We sincerely acknowledge and express our gratitude to the authors of the original GWAS for providing the data and their diligent efforts.

References

[1] Hoffeld K, Lenz M, Egenolf P, et al. Patient-related risk factors and lifestyle factors for lumbar degenerative disc disease: a systematic review[J]. Neurochirurgie, 2023, 69(5): 101482.
[2] Vos T, Barber R M, Bell B, et al. Global, regional, and national incidence, prevalence, and years lived with disability for 301 acute and chronic diseases and injuries in 188 countries, 1990–2013: a systematic analysis for the Global Burden of Disease Study 2013[J]. The Lancet, 2015, 386(9995): 743-800.
[3] Seidler A, Bolm-Audorff U, Siol T, et al. Occupational risk factors for symptomatic lumbar disc herniation: a case-control study[J]. Occupational and Environmental Medicine, 2003, 60(11): 821-830.
[4] Seidler A, Bergmann A, Jäger M, et al. Cumulative occupational lumbar load and lumbar disc disease – results of a German multi-center case-control study (EPILIFT)[J]. BMC Musculoskeletal Disorders, 2009, 10(1).
[5] Seidler A, Bolm-Audorff U, Heiskel H, et al. The role of cumulative physical work load in lumbar spine disease: risk factors for lumbar osteochondrosis and spondylosis associated with chronic complaints[J]. Occupational and Environmental Medicine, 2001, 58(11): 735-746.
[6] Ja S. Natural history and nonoperative treatment of lumbar disc herniation[J]. PubMed, 1996.
[7] Yu P, Mao F, Chen J, et al. Characteristics and mechanisms of resorption in lumbar disc herniation[J]. Arthritis Research & Therapy, 2022, 24(1): 205.
[8] Zhou M, Theologis A A, O'Connell G D. Understanding the etiopathogenesis of lumbar intervertebral disc herniation: From clinical evidence to basic scientific research[J]. JOR SPINE, 2024, 7(1).
[9] Suyama K, Sakai D, Watanabe M. The Role of IL-17-Mediated Inflammatory Processes in the Pathogenesis of Intervertebral Disc Degeneration and Herniation: A Comprehensive Review[J]. Frontiers in Cell and Developmental Biology, 2022, 10.
[10] Kim H, Hong J Y, Lee J, et al. IL-1β promotes disc degeneration and inflammation through direct injection of the intervertebral disc in a rat lumbar disc herniation model[J]. The Spine Journal, 2021, 21(6): 1031-1041.
[11] Bernstein I A, Malik Q, Carville S, et al. Low back pain and sciatica: summary of NICE guidance[J]. BMJ, 2017.
[12] Van Den Heuvel M M, Oei E H G, Bierma-Zeinstra S M A, et al. The Prevalence of Abnormalities in the Pediatric Spine on MRI: A Systematic Review and Meta-Analysis[J]. Spine, 2020, 45(18): E1185-E1196.
[13] Wang Z, Liu X, Gao K, et al. Clinical effects and biological mechanisms of exercise on lumbar disc herniation[J]. Frontiers in Physiology, 15 (2024): 1309663.
[14] Gugliotta M, Da Costa B R, Dabis E, et al. Surgical versus conservative treatment for lumbar disc herniation: a prospective cohort study[J]. BMJ Open, 2016, 6(12): e012938.
[15] Delgado-López P D, Rodríguez-Salazar A, Martín-Alonso J, et.al. Hernia discal lumbar: historia natural, papel de la exploración, timing de la cirugía, opciones de tratamiento y conflicto de intereses [J]. Neurocirugía, 2017, 28(3): 124-134.
[16] Peul W C, Van Houwelingen H C, Van Den Hout W B, et al. Surgery versus Prolonged Conservative Treatment for Sciatica[J]. New England Journal of Medicine, 2007, 356(22): 2245-2256.
[17] Lequin M B, Verbaan D, Jacobs W C H, et al. Surgery versus prolonged conservative treatment for sciatica: 5-year results of a randomised controlled trial[J]. BMJ Open, 2013, 3(5): e002534.
[18] Fjeld O R, Grøvle L, Helgeland J, et al. Complications, reoperations, readmissions, and length of hospital stay in 34,639 surgical cases of lumbar disc herniation[J]. The Bone & Joint Journal, 2019, 101-B(4): 470-477.
[19] Kreiner D S, Hwang S W, Easa J E, et al. An evidence-based clinical guideline for the diagnosis and treatment of lumbar disc herniation with radiculopathy[J]. The Spine Journal, 2014, 14(1): 180-191.
[20] Wu H, Wang S, Chen W, et al. Collagen IX gene polymorphisms and lumbar disc degeneration: a systematic review and meta-analysis[J]. Journal of Orthopaedic Surgery and Research, 2018, 13(1).
[21] De Luca P, De Girolamo L, Perucca Orfei C, et al. Vitamin D's Effect on the Proliferation and Inflammation of Human Intervertebral Disc Cells in Relation to the Functional Vitamin D Receptor Gene FokI Polymorphism[J]. International Journal of Molecular Sciences, 2018, 19(7): 2002.
[22] Wang Z, Guo Z, Wang X, et al. Assessing the causal relationship between sepsis and autoimmune:

ISSN 2618-1584 Vol. 7, Issue 6: 125-140, DOI: 10.25236/FMSR.2025.070616

a mendelian randomization study[J]. Shock, 2023.
[23] Miao H, Chen S, Ding R. Evaluation of the Molecular Mechanisms of Sepsis Using Proteomics[J]. Frontiers in Immunology, 2021, 12.
[24] Russell J A, Meyer N J, Walley K R. Use of Mendelian randomization to better understand and treat sepsis[J]. Intensive Care Medicine, 2022, 48(11): 1638-1641.
[25] Sekula P, Del Greco M F, Pattaro C, et al. Mendelian Randomization as an Approach to Assess Causality Using Observational Data[J]. Journal of the American Society of Nephrology, 2016, 27(11): 3253-3265.
[26] Sanderson E, Glymour M M, Holmes M V, et al. Mendelian randomization[J]. Nature Reviews Methods Primers, 2022, 2(1).
[27] Ferkingstad E, Sulem P, Atlason B A, et al. Large-scale integration of the plasma proteome with genetics and disease[J]. Nature Genetics, 2021, 53(12): 1712-1721.
[28] Do C, Shearer A, Suzuki M, et al. Genetic–epigenetic interactions in cis: a major focus in the post-GWAS era[J]. Genome Biology, 2017, 18(1).
[29] Yang J, Lee S H, Goddard M E, et al. GCTA: A Tool for Genome-wide Complex Trait Analysis[J]. The American Journal of Human Genetics, 2011, 88(1): 76-82.
[30] Chen Y, Lu T, Pettersson-Kymmer U, et al. Genomic atlas of the plasma metabolome prioritizes metabolites implicated in human diseases[J]. Nature Genetics, 2023, 55(1): 44-53.
[31] Birney E. Mendelian Randomization[J]. Cold Spring Harbor Perspectives in Medicine, 2021: a041302.
[32] Yuan S, Larsson S C. Coffee and Caffeine Consumption and Risk of Kidney Stones: A Mendelian Randomization Study[J]. American Journal of Kidney Diseases, 2022, 79(1).
[33] Zhang L, Xiong Y, Zhang J, et al. Systematic proteome-wide Mendelian randomization using the human plasma proteome to identify therapeutic targets for lung adenocarcinoma[J]. Journal of Translational Medicine, 2024, 22(1).
[34] Burgess S, Thompson S G, CRP CHD Genetics Collaboration. Avoiding bias from weak instruments in Mendelian randomization studies[J]. International Journal of Epidemiology, 2011, 40(3): 755-764.
[35] Xin J, Jiang X, Ben S, et al. Correction: Association between circulating vitamin E and ten common cancers: evidence from large-scale Mendelian randomization analysis and a longitudinal cohort study[J]. BMC Medicine, 2022, 20(1).
[36] Li C, Deans N C, Buell C R. "Simple Tidy GeneCoEx": A gene co-expression analysis workflow powered by tidyverse and graph-based clustering in R[J]. The Plant Genome, 2023, 16(2).
[37] Korthauer K, Kimes P K, Duvallet C, et al. A practical guide to methods controlling false discoveries in computational biology[J]. Genome Biology, 2019, 20(1).
[38] Verbanck M, Chen C Y, Neale B, et al. Detection of widespread horizontal pleiotropy in causal relationships inferred from Mendelian randomization between complex traits and diseases[J]. Nature Genetics, 2018, 50(5): 693-698.
[39] Wu F, Huang Y, Hu J, et al. Mendelian randomization study of inflammatory bowel disease and bone mineral density[J]. BMC Medicine, 2020, 18(1).
[40] Chen X, Hong X, Gao W, et al. Causal relationship between physical activity, leisure sedentary behaviors and COVID-19 risk: a Mendelian randomization study[J]. Journal of Translational Medicine, 2022, 20(1).
[41] Magkrioti C, Galaris A, Kanellopoulou P, et al. Autotaxin and chronic inflammatory diseases[J]. Journal of Autoimmunity, 2019, 104: 102327.
[42] Sevastou I, Kaffe E, Mouratis M A, et al. Lysoglycerophospholipids in chronic inflammatory disorders: The PLA2/LPC and ATX/LPA axes[J]. Biochimica et Biophysica Acta (BBA) - Molecular and Cell Biology of Lipids, 2013, 1831(1): 42-60.
[43] Fulkerson Z, Wu T, Sunkara M, et al. Binding of Autotaxin to Integrins Localizes Lysophosphatidic Acid Production to Platelets and Mammalian Cells[J]. Journal of Biological Chemistry, 2011, 286(40): 34654-34663.
[44] Leblanc R, Lee S C, David M, et al. Interaction of platelet-derived autotaxin with tumor integrin αVβ3 controls metastasis of breast cancer cells to bone[J]. Blood, 2014, 124(20): 3141-3150.
[45] Hausmann J, Kamtekar S, Christodoulou E, et al. Structural basis of substrate discrimination and integrin binding by autotaxin[J]. Nature Structural & Molecular Biology, 2011, 18(2): 198-204.
[46] Uranbileg B, Ito N, Kurano M, et al. Inhibition of autotaxin activity ameliorates neuropathic pain derived from lumbar spinal canal stenosis[J]. Scientific Reports, 2021, 11(1).
[47] Menezes J, Jakobsson J E, Bersellini Farinotti A, et al. Comparative Analysis of Lysophosphatidic Acid Levels in Fibromyalgia and Other Painful Conditions in Female Patients[J]. European Journal of Pain, 2025, 29(6).
[48] Bernabucci M, Notartomaso S, Zappulla C, et al. N-Acetyl-Cysteine Causes Analgesia by

ISSN 2618-1584 Vol. 7, Issue 6: 125-140, DOI: 10.25236/FMSR.2025.070616

Reinforcing the Endogenous Activation of Type-2 Metabotropic Glutamate Receptors[J]. Molecular Pain, 2012, 8: 1744-8069-8-77.
[49] Heidari B, Seyedian Z A, Mehrpooya M, et al. N-Acetyl Cysteine as an Add-on Therapy is Useful in Treating AcuteLumbar Radiculopathy Caused by Disc Herniation: Results of aRandomized, Controlled Clinical Trial[J]. Reviews on Recent Clinical Trials, 2023, 18(4): 288-299.
[50] Chen X, Zhang A, Zhao K, et al. The role of oxidative stress in intervertebral disc degeneration: Mechanisms and therapeutic implications[J]. Ageing Research Reviews, 2024, 98: 102323.
[51] Zhang Q, Li J, Li Y, et al. BMI deficiency causes oxidative stress and intervertebral disc degeneration, which can be alleviated by antioxidant treatment[J]. Journal of Cellular and Molecular Medicine, 2020, 24(16): 8950-8961.
[52] Wu S, Shi Y, Jiang L, et al. N -Acetylcysteine-Derived Carbon Dots for Free Radical Scavenging in Intervertebral Disc Degeneration[J]. Advanced Healthcare Materials, 2023, 12(24): 2300533.
[53] Ai J, Wan H, Shu M, et al. Guhong injection protects against focal cerebral ischemia–reperfusion injury via anti-inflammatory effects in rats[J]. Archives of Pharmacal Research, 2017, 40(5): 610-622.
[54] Xu S, Li C, Zhou H, et al. A Study on Acetylglutamine Pharmacokinetics in Rat Blood and Brain Based on Liquid Chromatography-Tandem Mass Spectrometry and Microdialysis Technique[J]. Frontiers in Pharmacology, 2020, 11: 508.
[55] Granger A J, Mulder N, Saunders A, et al. Cotransmission of acetylcholine and GABA[J]. Neuropharmacology, 2016, 100: 40-46.
[56] Sun Z, Jin H, Zhou H, et al. Guhong Injection promotes fracture healing by activating the Wnt/beta-catenin signaling pathway in vivo and in vitro[J]. Biomedicine & Pharmacotherapy, 2019, 120: 109436.
[57] Wu L, Chen S, He B, et al. Acetylglutamine facilitates motor recovery and alleviates neuropathic pain after brachial plexus root avulsion in rats[J]. Journal of Translational Medicine, 2023, 21(1): 563.
[58] Levi S, Corsi B, Bosisio M, et al. A Human Mitochondrial Ferritin Encoded by an Intronless Gene[J]. Journal of Biological Chemistry, 2001, 276(27): 24437-24440.
[59] Santambrogio P, Biasiotto G, Sanvito F, et al. Mitochondrial Ferritin Expression in Adult Mouse Tissues[J]. Journal of Histochemistry & Cytochemistry, 2007, 55(11): 1129-1137.
[60] Nie G, Sheftel A D, Kim S F, et al. Overexpression of mitochondrial ferritin causes cytosolic iron depletion and changes cellular iron homeostasis[J]. Blood, 2005, 105(5): 2161-2167.
[61] Campanella A, Rovelli E, Santambrogio P, et al. Mitochondrial ferritin limits oxidative damage regulating mitochondrial iron availability: hypothesis for a protective role in Friedreich ataxia[J]. Human Molecular Genetics, 2008, 18(1): 1-11.
[62] Yang Q, Nausch L W M, Martin G, et al. Crystal Structure of Human Poly(A) Polymerase Gamma Reveals a Conserved Catalytic Core for Canonical Poly(A) Polymerases[J]. Journal of Molecular Biology, 2014, 426(1): 43-50.
[63] Topalian S L, Kaneko S, Gonzales M I, et al. Identification and Functional Characterization of Neo-Poly(A) Polymerase, an RNA Processing Enzyme Overexpressed in Human Tumors[J]. Molecular and Cellular Biology, 2001, 21(16): 5614-5623.
[64] Liao Y, Chen Q, Wang H, et al. SARS-CoV-2-Induced PAPOLG Contributes to Inflammation Response by Stabilizing NF-κB mRNA[J]. Journal of Medical Virology, 2025, 97(7).
[65] Bonagurio L P, Murakami A E, Moreira C A, et al. Dietary supplementation with inosine-5'-monophosphate improves the functional, energetic, and antioxidant status of liver and muscle growth in pigs[J]. Scientific Reports, 2022, 12(1): 350.
[66] Kinnamon S C. Umami taste transduction mechanisms[J]. The American Journal of Clinical Nutrition, 2009, 90(3): 753S-755S.
[67] Zhang B, Xu Y, Liu J, et al. Oral Intake of Inosine 5'-Monophosphate in Mice Promotes the Absorption of Exogenous Fatty Acids and Their Conversion into Triglycerides through Enhancing the Phosphorylation of Adenosine 5'-Monophosphate-Activated Protein Kinase in the Liver, Leading to Lipohyperplasia[J]. International Journal of Molecular Sciences, 2023, 24(19): 14588.
[68] Takahashi H, Tokura M, Kawarasaki S, et al. Metabolomics reveals inosine 5'-monophosphate is increased during mice adipocyte browning[J]. Journal of Biological Chemistry, 2022, 298(10): 102456.
[69] Shiri R, Lallukka T, Karppinen J, et al. Obesity as a Risk Factor for Sciatica: A Meta-Analysis[J]. American Journal of Epidemiology, 2014, 179(8): 929-937.